Received: March 29, 2025. Revised: April 29, 2025.

INASS

International Journal of
Intelligent Engineering & Systems

http://www.inass.org/

Adaptive Frilled Lizard Optimization for Enhancing Distribution Feeder Performance with Renewables and Charging Stations

Srinivasarao Thumati[1]* Veera Reddy Aduru[2] Imran Abdul[3] Ramakrishna Guttula[4] Janjhyam Venkata Naga Ramesh[5,6] Linginedi Ushasree[7]

[1]*Prasad V. Potluri Siddhartha Institute of Technology, Vijayawada-520007, Andhra Pradesh, India*
[2]*Siddhartha Academy of Higher Education (Deemed to be University), Vijayawada-520007, Andhra Pradesh, India*
[3]*Lakireddy Bali Reddy College of Engineering, Mylavaram, Krishna-521230, Andhra Pradesh, India*
[4]*Aditya University, Surampalem -533437, Andhra Pradesh, India*
[5]*Graphic Era Hill University, Dehradun, 248002, Uttarakhand, India*
[6]*Graphic Era Deemed to be University, Dehradun, 248002, Uttarakhand, India*
[7]*Koneru Lakshmaiah Education Foundation, Vaddeswaram, Guntur Dist., Andhra Pradesh - 522302, India*
Corresponding author's Email: srinuthumati@gmail.com

Abstract: The growing integration of renewable energy sources and electric vehicle (EV) fast-charging stations (FCSs) in power distribution networks introduces challenges such as increased power losses, voltage instability, and operational complexity. To address these issues, this study proposes Adaptive Frilled Lizard Optimization (A-FLO), an enhanced metaheuristic algorithm inspired by the predatory behaviour of frilled lizards. Unlike conventional optimizers with static control parameters, A-FLO introduces adaptive mechanisms that dynamically adjust exploration and exploitation strategies through modified hunting and climbing behaviours. A-FLO is employed to optimize the placement and sizing of distributed generators (DGs) and FCSs in electrical distribution networks (EDNs) under high EV penetration. The results demonstrate that A-FLO effectively reduces power losses, improves voltage profiles, and enhances voltage stability in IEEE 33-bus, 69-bus and 118-bus EDNs. Comparative evaluations with recent metaheuristic algorithms confirm A-FLO's superior convergence reliability, solution quality, and scalability. The proposed method shows strong potential for real-world smart grid applications involving the coordinated planning of renewable energy and EV infrastructure.

Keywords: Adaptive frilled lizard optimization, Distributed generators, Fast-charging stations, Electric vehicle penetration, Voltage stability improvement, Smart grid optimization.

1. Introduction

The integration of renewable energy sources and electric vehicle (EV) charging stations in distribution networks presents challenges such as power losses, voltage instability, and increased operational complexity [1, 2]. Effective planning and optimization strategies are essential for enhancing system performance while ensuring sustainability. Recent research highlights the importance of advanced algorithms in determining the optimal placement of charging stations and renewable energy sources [3]. Several studies have focused on the optimal integration of charging stations using different metaheuristic approaches. In [4], a hybrid gray wolf optimization particle swarm optimization (GWOPSO) was proposed for multi-objective EV charging station (CS) placement. The solution improved power quality and grid reliability but lacked real-world validation and integration with renewable energy sources. Similarly, [5] developed a stochastic power flow model for optimal EV charging station siting and sizing, enhancing voltage stability using adaptive differential evolution optimization algorithm (ADEOA). However, it did not consider dynamic EV demand variations and real-time optimization. In [6], a modified

Archimedes optimization algorithm (MAOA) was introduced for CS placement. While it improved computational efficiency, it did not address uncertainties in renewable energy generation and charging station load variations. Likewise, [7] focused on reliable CS allocation using galaxy gravity optimization (GGO). Further, a comprehensive review analyzed challenges, mitigation approaches, and optimization strategies for CS infrastructure [8].

Further research has explored various optimization strategies for integrating EV CSs and renewable distribution generation (DGs) into electrical distribution networks (EDNs). Recently, [9] proposed direct search (DS) with PSO (PSO-DS) for optimal CS and capacitor banks (CBs) allocation focusing on real power loss and voltage profile. In [10], PSO with backward-forward sweep load flow is introduced for CS and DG allocation towards loss reduction and voltage profile improvement. The approach minimized power losses but did not address bidirectional energy flow challenges in vehicle-to-grid operations. In [11], a political optimization algorithm (POA) was applied for the optimal allocation of DGs and EVs in a EDN. A multi-objective dragonfly algorithm (MODA) based allocation strategy for CSs and renewable DGs were proposed in [12], incorporating demand response (DR). In [13], improved bald eagle search (IBES) algorithm was proposed for the optimal deployment of EV fast charging stations (FCSs) alongside solar-based DGs. The method improved system reliability and power quality, yet it did not fully address the computational complexity and scalability of AI-driven solutions. The study in [14] applied the African vulture optimization algorithm (AVOA) for optimal placement of DSTATCOM and DG to minimize the impact of EV charging on radial distribution networks (RDNs). However, it lacked dynamic load forecasting and adaptive control mechanisms. In [15], the placement of CSs and RDGs was explored considering uncertainties using Harris hawks optimization (HHO). While it improved network reliability, it did not fully account for demand-side management strategies and real-time power fluctuations. In [16], the bald eagle search algorithm (BSA) was applied for optimal integration of EV CSs and DSTATCOM in Indian distribution systems. In [17], an enhanced pathfinder algorithm (EPFA) was used for the optimal integration of solar photovoltaics (SPVs) and rapid charging stations (RCSs) in low-voltage RDNs. The method minimized power losses but did not fully address uncertainties in solar power generation and EV demand. The study in [18] employed the arithmetic optimization algorithm (AOA) for EV charging station placement to minimize line losses. It enhanced grid efficiency but lacked a comparative analysis with other metaheuristic approaches. In [19], a techno-economic assessment was conducted for grid and renewable-powered CSs in India using a modified salp swarm algorithm (MSSA). The approach improved cost-effectiveness but did not incorporate vehicle-to-grid (V2G) interactions. In [20], the hunter–prey optimization (HPO) is introduced for the optimal allocation of PV, DSTATCOM, and CSs in RDNs. While it enhanced power quality and voltage profiles, it did not evaluate large-scale distribution networks with high EV penetration. In [21], an improved pufferfish optimization algorithm (IPOA) was introduced for the optimal allocation of PV-FCSs in RDNs. The method enhanced power loss reduction and voltage stability but lacked a comparative analysis with emerging optimization techniques. In [22], arithmetic optimization algorithm (AOA) is employed for solaving DGs and CBs by aiming loss reduction, voltage profile improvement and voltage stability enhancement. In [23], multi-objective whale optimization (MOWOA) based DGs are optimally integrated for improving the RDNs performance. Further, the integration of DGs and EVs in power systems was reviewed, highlighting challenges related to grid stability and energy management [24, 25].

In previous studies as summarised in Table 1, metaheuristics have been shown to optimize CS and DG placement in EDNs. However, many of these algorithms prematurely converge, trapping them in local optima. Researchers hybridize current approaches or design new algorithms with improved exploration and exploitation to improve optimization performance [26]. Frilled Lizard Optimization (FLO) [27], a new algorithm, simulates frilled lizard hunting in the wild. This study implements FLO to integrate CS and DGs in EDNs and compares it to metaheuristic algorithms using IEEE 33, 69, and 85-bus EDN simulations. Further, the suggested adaptive-FLO (A-FLO) is modelled frilled lizard predatory and defensive instincts to dynamically change its search behaviour, unlike most metaheuristics that focus on exploration or exploitation with set control parameters. Its adaptive hunting and climbing tactics balance global search with local refining over time, reducing premature convergence and increasing solution variety.

A-FLO may go from broad exploration to concentrated exploitation, unlike IPOA, PSO, and

Table 1. Comparisons of literature in terms of optimization schemes and performance indices

Method	**Optimization schemes**			**Performance assessment**					**Grid Size**
	CS	CS+DG	DR	Loss	AVDI	VSI	Cost	Reliability	
GWOPSO [4]	✓	–	–	✓	✓	✓	–	–	34-bus
ADEOA [5]	✓	–	–	–	–	✓	✓	–	33-bus
MAOA [6]	✓	–	–	✓	✓	✓	–	–	33, 69 & 10-bus
GGO [7]	✓	✓	–	✓	–	–	✓	✓	69-bus
PSO-DS [9]	✓	✓	–	✓	✓	–	–	–	33-bus
PSO [10]	✓	✓	–	✓	✓	–	–	–	33-bus
POA [11]	✓	✓	–	✓	✓	✓	–	–	28-bus
MODA [12]	✓	✓	✓	✓	✓	✓	✓	✓	69-bus
IBES [13]	✓	✓	–	✓	✓	✓	✓	✓	UEN (30-bus)
AVOA [14]	✓	✓	–	✓	✓	✓	–	–	33, 69 & 136-bus
HHO [15]	✓	✓	–	✓	✓	–	✓	✓	33-bus
BES [16]	✓	✓	–	✓	✓	✓	✓	–	28 & 108-bus
EPFA [17]	✓	✓	–	✓	✓	✓	–	–	69-bus
AOA [18]	✓	✓	–	✓	✓	–	–	–	33-bus
MSSA [19]	✓	✓	–	–	–	–	✓	–	New Delhi
HPO [20]	✓	✓	–	✓	✓	✓	–	–	33, 69 & 136-bus
IPOA [21]	✓	✓	–	✓	✓	–	–	–	33 & 69-bus
AOA [22]	✓	✓	–	✓	✓	–	–	–	33 & 69-bus
MOWOA [23]	–	✓	–	✓	✓	–	–	–	33 & 69-bus
Proposed	✓	✓	–	✓	✓	✓	–	–	33 & 69-bus

Table 2. Comparison of A-FLO in solving 13 benchmark engineering problems

Problem	**HHO**			**FLO**			**A-FLO**		
	Best	Mean	Std	Best	Mean	Std	Best	Mean	Std
EP1	2994.426	2999.659	5.017	2994.425	2999.004	5.514	2994.424	2998.813	4.5
EP2	0.013	0.013	0	0.013	0.013	0	0.013	0.013	0
EP3	6059.714	6241.665	267.138	6059.714	6247.732	282.551	6059.714	6229	250
EP4	263.896	263.896	0	263.896	263.896	0	263.896	263.896	0
EP5	0	0	0	0	0	0	0	0	0
EP6	1.34	1.398	0.185	1.34	1.361	0.055	1.34	1.345	0.075
EP7	0.013	0.013	0	0.013	0.013	0	0.013	0.013	0
EP8	26.486	26.486	0	26.486	26.486	0	26.486	26.486	0
EP9	8.413	108.241	102.215	8.413	125.329	75.397	8.413	115	70
EP10	6.843	6.843	0	6.843	6.843	0	6.843	6.843	0
EP11	22.868	23.558	0.545	22.844	23.713	0.692	22.888	23.48	0.48
EP12	1.725	1.742	0.065	1.725	1.726	0.003	1.725	1.73	0.01
EP13	359.208	359.208	0	359.208	359.208	0	359.208	359.2	0.1

other single-strategy optimizers. This makes A-FLO ideal for non-linear, multi-constrained power system optimization issues, as shown by its higher performance on benchmark test systems. The following are the major contributions of this research work.

- Developed a novel bio-inspired algorithm for optimal placement of EV charging stations and renewable energy resources in distribution networks, improving efficiency and stability.
- Improved voltage stability, minimized power losses, and enhanced network resilience by dynamically balancing exploration and exploitation strategies in optimization.
- Demonstrated A-FLO's superiority over existing metaheuristic algorithms through simulations on IEEE 33-bus, 69-bus and 118-bus test systems, ensuring scalability and adaptability.

- Addressed limitations of conventional approaches by reducing premature convergence and local optima trapping, making A-FLO suitable for real-world smart grid applications.

Structure of the paper's remainder: Section 2 covers theoretical notions and modeling. The problem formulation and objective functions and restrictions for optimal placement are in Section 3. The adaptive hunting and climbing tactics of the A-FLO algorithm are described in Section 4. Section 5 compares A-FLO to other optimization techniques using IEEE EDNs. Section 6 summarizes major data, highlights A-FLO's benefits, and suggests grid optimization research directions.

2. Modelling of CS and DG impact

The CS is treated as a lumped load on the power grid. When CSs are integrated into the system, additional loads are introduced due to charging demand of EVs. Further, by integrating a renewable DG, the loading condition can be offset by the equivalent of its power generation. Thus, the new total load at bus *j* with a CS/DG can be written as,

$$P_j^{new} = P_j^{old} + P_{CS,j} - P_{DG,j} \quad (1)$$

$$Q_j^{new} = Q_j^{old} + Q_{CS,j} - Q_{DG,j} \quad (2)$$

$$Q_{CS,j} = P_{CS,j} \cdot tan(\emptyset_{ev,i}) \quad (3)$$

$$Q_{DG,j} = P_{DG,j} \cdot tan(\emptyset_{dg,i}) \quad (4)$$

3. Problem formulation

The placement of CS and RDGs in a power distribution system involves optimizing multiple electrical parameters to ensure efficient operation, minimize losses, and enhance voltage stability.

$$P_{loss} = \sum_{i=1}^{N} \rho_i \left(\frac{|S_i|^2}{|V_i|^2}\right) \quad (5)$$

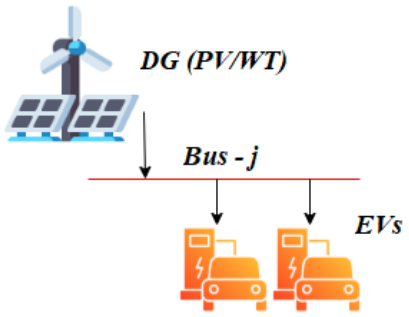

Fig. 1. Illustration of CS and DG integration at a distribution bus-*j*

Further, the impact of CS and DGs is analysed on feeder voltage profile and voltage stability, and are given by,

$$AVDI = \frac{1}{N}\sum_{i=1}^{N}|V_i - V_r| \quad (6)$$

$$v_{SI} = \sum_{i=1}^{N_{br}} \frac{4Z_i P_i}{|V_i|^2} \quad (7)$$

The following are the constraints considered while optimizing the objective function.

$$V_{min} \le |V_i| \le V_{max}, \forall i \in N_{bus} \quad (8)$$

$$0 \le P_{CS,i} \le P_{CS}^{max}, \forall i \in N_{CS} \quad (9)$$

$$P_{D,new} = P_{D,base} + P_{loss} + P_{CS} - P_{DG} \quad (10)$$

$$Q_{D,new} = Q_{D,base} + Q_{loss} + Q_{CS} - Q_{DG} \quad (11)$$

4. Proposed solution methodology

A new bio-inspired metaheuristic called Frilled Lizard Optimization (FLO) imitates the predatory and defensive tendencies of the frilled lizard are introduced as a solution technique in this work.

4.1 Frilled lizard optimization

There are two main stages to the FLO approach. Exploration (hunting strategy): The lizard's capacity to search globally is improved by its quick approach to prey. After feeding, the lizard withdraws to a tree and refines its solutions in the local search space, a behaviour known as exploitation (tree climbing).

4.1.1. Initialization

The initial population of frilled lizards is randomly generated within the defined search bounds:

$$X_{i,d} = lb_d + r \cdot (ub_d - lb_d) \quad (12)$$

where $r \sim U(0,1)$ is the uniformly distributed random number, lb_d and ub_d are the lower and upper bounds of the search space in dimension d, respectively.

$$F_i = F(X_i), i = 1,2,\ldots,N \quad (13)$$

4.1.2. Hunting strategy

During hunting, the frilled lizard selects a prey from a subset of solutions that have better objective

function values and the lizard moves toward its prey, given by:

$$L_i = \{x_k | F(x_k) < F(x_i), k \neq i\} \quad (14)$$

$$x_i' = x_i + \alpha \cdot r \cdot (x_p - x_i) - \beta \cdot I \cdot x_i \quad (15)$$

where α and β are the exploration coefficients, I is a randomly chosen intensity factor from {1,2}, $r \sim U(0,1)$ is a random factor to diversify search. The new position is updated as:

$$x_i = \begin{cases} x_i' & if\ F(x_i') < F(x_i) \\ x_i & otherwise \end{cases} \quad (16)$$

4.1.3. Climbing to safety

After feeding, the frilled lizard climbs a nearly tree to refine its position. The position is updated based on the new function evaluation and are given by:

$$x_i^{new} = x_i + (1 - 2r) \cdot \gamma \cdot (ub_d - lb_d) \quad (17)$$

where γ is the exploration decay factor that reduces as iterations progress, $(1 - 2r)$ ensures movement in both directions within bounds.

$$x_i = \begin{cases} x_i^{new} & if\ F(x_i^{new}) < F(x_i) \\ x_i & otherwise \end{cases} \quad (18)$$

The process continues iteratively until the stopping criterion is met (maximum iterations *T* or convergence to a threshold solution). The best solution found is:

$$X_{best} = \underset{x_i}{\arg min}\, F(x_i), i \in \{1, \ldots, N\} \quad (19)$$

By combining climbing (intensification) and hunting behaviour (diversification), FLO effectively strikes a balance between phases of exploration and exploitations.

4.2 Adaptive frilled lizard optimization

A dynamic exploration coefficient $\lambda(t)$ is introduced as defined in Eq. (20) and the changes in Eq. (21). This ensures that initial iterations favour exploration, while later iterations prioritize exploitation.

$$\lambda(t) = e^{-\phi \cdot \frac{t}{T}} \quad (20)$$

$$x_i' = x_i + \lambda(t) \cdot r_1 \cdot (x_p - x_i) - \{1 - \lambda(t)\} \cdot r_2 \cdot (x_i - X_{best}) \quad (21)$$

where x_p randomly chosen prey from L_i , $\lambda(t)$ determines how much random exploration is allowed, X_{best} ensures attraction towards the best solution, $r_1, r_2 \sim U(0,1)$ are random weights. This adaptive movement reduces randomness over time, shifting from broad exploration to fine-tuned search.

Once the lizard feeds, it moves up a tree to refine its position. The movement strategy here is refined by the adaptive exploitation factor $\mu(t)$.

$$\mu(t) = 1 - e^{-\phi \cdot \frac{t}{T}} \quad (22)$$

$$x_i^{new} = x_i + \mu(t) \cdot (1 - 2r) \cdot (ub_d - lb_d) \quad (23)$$

where$\mu(t)$ increases over time to favour exploration, $(1 - 2r)$ ensures movement in both positive and negative directions.

These adaptive hunting strategy and adaptive climbing strategy enhance exploration-exploitation dynamically, promoting convergence without premature stagnation, enhancing global search in early iterations and improving local search in later iterations.

4.3 Performance analysis of A-FLO

The A-FLO's effectiveness was evaluated using 13 benchmark engineering design problems. The best function values obtained by A-FLO are described here.

EP1. *Speed Reducer* – Achieved a best fitness of 2994.424, reflecting an efficient mechanical design.

EP2. *Tension/Compression Spring Design* – Resulted in a minimal fitness of 0.013, indicating a highly optimized spring configuration.

EP3. *Pressure Vessel Design* – Recorded a best fitness of 6059.714, accounting for cost and structural constraints.

EP4. *Three-Bar Truss Design* – Attained a fitness of 263.896, balancing material use and stress limits.

EP5. *Design of Gear Train* – Perfect optimization with a best fitness of 0.000, signifying an ideal solution.

EP6. *Cantilever Beam* – Yielded a best fitness of 1.340, minimizing weight while maintaining strength.

EP7. *Minimize I-Beam Vertical Deflection* – Achieved 0.013, showing minimal deflection.

EP8. *Tubular Column Design* – Reached a fitness of 26.486, optimizing cross-sectional parameters.
EP9. *Piston Lever* – Best fitness of 8.413, targeting efficient load transfer.
EP10. *Corrugated Bulkhead Design* – Recorded 6.843, optimizing for structural efficiency.
EP11. *Car Side Impact Design* – Achieved 22.888, focusing on safety and material constraints.
EP12. *Design of Welded Beam* – Obtained 1.725, balancing stress and fabrication cost.
EP13. *Reinforced Concrete Beam Design* – Best fitness of 359.208, meeting strength and economy requirements.

In Table 2, the performance analysis across 13 engineering design problems demonstrates that A-FLO consistently achieves superior optimization results compared to both HHO and FLO. It records the lowest mean fitness and standard deviation in most cases, indicating not only high-quality solutions but also enhanced stability and robustness. HHO, while not outperforming A-FLO, performs better than FLO in several problems, showcasing improved reliability over the original FLO approach. FLO, although occasionally competitive in best-case fitness, generally falls behind in terms of average performance and consistency. These findings affirm that A-FLO offers a balanced and reliable optimization capability, making it the most effective algorithm for diverse engineering applications under this comparative study.

5. Simulation results

Simulations are carried out on IEEE standard test systems under various operational scenarios using custom-developed programs in MATLAB R2023b. The computational experiments are executed on a personal computer configured with an Intel® Core™ i7-8750 CPU @ 2.20 GHz and 16 GB RAM, ensuring reliable performance and efficient processing of optimization routines.

5.1 Scenario-1 (Base case)

In this scenario, the test systems are assumed to be serving only feeder regular load and not integrated with any DGs and CSs. The analysis of the 33-bus and 69-bus distribution systems in Table 3 reveals key performance metrics related to power generation, load demand, power losses, and voltage stability.

In the 33-bus system, generation is 3926.00 kW and 2443.03 kVAr, supplying 3715.00 kW and 2300.00 kVAr load, with losses of 210.998 kW and 143.033 kVAr. The minimum voltage is 0.9038 p.u. at bus 18. AVDI and VSI are 0.6486 and 0.0111, indicating moderate voltage deviation and acceptable stability.

For the 69-bus system, generation is 4027.10 kW and 2796.86 kVAr for a load of 3802.10 kW and 2694.70 kVAr, with 225.001 kW and 102.165 kVAr losses. The lowest voltage is 0.9092 p.u. at bus 65. AVDI is 0.5500 and VSI is 0.0046, reflecting higher voltage deviation and lower stability than the 33-bus system.

5.2 Scenario-2 (With EV load penetration)

In Table 4, with 50% EV load penetration, the 33-bus and 69-bus distribution systems exhibit significant changes in power demand, losses, and voltage stability compared to the base case.

In the 33-bus system, generation rises to 5202.49 kW and 3181.98 kVAr, meeting a higher load of 4866.10 kW and 2955.33 kVAr. Losses grow to 336.39 kW and 226.65 kVAr. The minimum voltage drops from 0.9038 p.u. to 0.8793 p.u. at bus 18, AVDI decreases from 0.6486 to 0.5767, indicating worsened voltage deviation, while VSI improves slightly from 0.0111 to 0.0139.

In the 69-bus system, generation increases to 5379.66 kW and 3548.54 kVAr for a load of 5034.29 kW and 3388.56 kVAr. Losses escalate to 345.38 kW and 159.98 kVAr. The minimum voltage falls from 0.9092 p.u. to 0.8888 p.u. at bus 65, AVDI declines from 0.5500 to 0.4713, while VSI slightly improves from 0.0046 to 0.0057.

5.3 Scenario-3 (With CSs)

With the optimal placement of three fast charging stations (FCSs), both the 33-bus and 69-bus systems show marked improvements in operational performance under 50% EV penetration compared to non-optimized scenarios.

In the 33-bus system, FCSs are optimally located at buses 2, 19, and 26 with respective supplies of 500 kW, 400 kW, and 300 kW. This integration reduces active and reactive power generation from 5202.49 kW/ 3181.98 kVAr to 5165.52 kW/ 2861.70 kVAr. Losses drop significantly: real power loss from 336.39 kW to 250.52 kW and reactive power loss from 226.65 kVAr to 167.28 kVAr. Voltage performance also improves, with Vmin increasing from 0.8793 p.u. to 0.8973 p.u., and AVDI rising from 0.5767 to 0.6300, indicating better voltage regulation. A slight drop in VSI from 0.0139 to 0.01199 suggests a minor trade-off in stability.

In the 69-bus system, FCSs at buses 2, 28, and 47 (500 kW, 400 kW, 300 kW) help reduce generation from 5379.66 kW/3548.54 kVAr to 5227.22 kW/ 3191.57 kVAr. Real and reactive losses decline from 345.38 kW/ 159.98 kVAr to 225.12 kW/ 102.45 kVAr, approaching pre-EV levels. Vmin improves from 0.8888 p.u. to 0.9092 p.u., while AVDI increases from 0.4713 to 0.54998. The VSI stabilizes at 0.0046, matching the original value, reflecting restored voltage stability.

5.4 Scenario-4 (With CSs and DGs)

With the integration of photovoltaic (PV) units alongside optimally placed fast charging stations (FCSs), both the 33-bus and 69-bus systems exhibit significant improvements in efficiency, voltage profile, and system stability compared to the scenario with only FCS integration under 50% EV load penetration.

In the 33-bus system, PV units installed at buses 30, 13, and 24 (with capacities of 1305.36 kW, 966.70 kW, and 1514.05 kW, respectively) substantially reduce the active power generation from 5165.52 kW to 1217.27 kW and reactive generation from 2861.70 kVAr to 2755.60 kVAr. Real and reactive losses are minimized from 250.52 kW and 167.28 kVAr to 88.27 kW and 61.17 kVAr, respectively. The minimum voltage improves from 0.8973 p.u. to 0.9743 p.u., shifting from bus 18 to bus 33, and the AVDI increases from 0.6300 to 0.8222, indicating better voltage regulation. Although the VSI slightly drops from 0.01199 to 0.00298, the overall system becomes more stable and efficient.

In the 69-bus system, PV units at buses 12, 9, and 22 (354.65 kW, 372.66 kW, and 408.09 kW) help lower the active power generation from 5227.22 kW to 4049.42 kW and reactive generation from 3191.57 kVAr to 3171.16 kVAr. Real and reactive losses reduce from 225.12 kW and 102.45 kVAr to 183.32 kW and 82.04 kVAr, respectively. The minimum voltage increases from 0.9092 p.u. to 0.9165 p.u. at bus 65. AVDI improves from 0.54998 to 0.5703, and VSI enhances from 0.0046 to 0.00355, reflecting a stronger voltage stability margin.

5.5 Comparative study

The computational efficacy of A-FLO is compared for Scenario-3 with literature works are reported in Table 7. The performance of IPOA [21], AOA [22], and A-FLO was evaluated on the IEEE 33-bus in terms of minimizing Ploss through optimal DG placement at buses 13, 24, and 30. IPOA achieved a Ploss of 72.79 kW with DGs sized at 801.7, 1091.33, and 1053.64 kW. AOA provided similar loss (72.79 kW) with slightly altered sizes. A-FLO optimized DGs are 1091.304 kW (bus 13), 801.349 kW (bus 24), and 1054.11 kW (bus 30), and thus, Ploss reduced marginally to 72.787 kW, highlighting its efficient allocation strategy.

For the IEEE 69-bus, IPOA [21], AOA [22], EPFA [17], and A-FLO were compared for DG placement at key buses. IPOA achieved the best performance with a Ploss of 69.4262 kW using DGs at buses 11 (526.75 kW), 18 (380.43 kW), and 61 (1718.97 kW). AOA [22] and EPFA [17] yielded similar losses (69.43 kW) with different bus allocations. A-FLO assigned 527.054 kW, 379.53 kW, and 1719.428 kW to buses 11, 18, and 61 respectively, resulting in a slightly lower loss of 69.428 kW.

Further, the efficacy of A-FLO is analyzed on the larger-scale IEEE 118-bus and compared with the FLO, Harris Hawks Optimization (HHO) [28], Hiking Optimization Algorithm (HOA) [29], and Polar Lights Optimizer (PLO) [30] for solving DG allocation (Scenario-3). For each algorithm, the population size and maximum number of iterations are set to 30 and 50, respectively. Additionally, 50 independent runs are performed.

In Table 8, the performance of HHO, HOA, PLO, and A-FLO is summarized on the IEEE 118-bus EDN for the DG allocation problem under Scenario-3. A-FLO outperforms other algorithms with the lowest real power loss (617.50 kW) and reactive power loss (455.49 kVAr). The optimal sizes are 3120.14 kW/ bus-109, 2519.27 kW/ bus-79, 2883.59 kW/ bus-50 and 2857.87 kW/ bus-71, resulted for total DG capacity of 11380.89 kW. It also shows the best minimum voltage magnitude (0.954 p.u. at bus 54) and the smallest AVDI (0.00072), indicating superior voltage profile regulation. VSI remains consistent across algorithms, with A-FLO and HHO showing a slightly better index (0.6557).

Table 3. Base case performance (Scenario-1)

System	P_{loss}	Q_{loss}	$AVDI$	VSI
33-bus	210.998	143.033	0.6486	0.0111
69-bus	225.001	102.165	0.5500	0.0046

Table 4. Performance with EV load (Scenario-2)

System	P_{loss}	Q_{loss}	$AVDI$	VSI
33-bus	336.392	226.651	0.57671	0.0139
69-bus	345.376	159.977	0.47126	0.0057

Table 5. Performance with CSs (Scenario-3)

System	P_{loss}	Q_{loss}	*AVDI*	*VSI*
33-bus	250.516	167.283	0.6300	0.0120
69-bus	225.124	102.446	0.5500	0.0046

Table 6. Performance with CSs and DGs (Scenario-4)

System	P_{loss}	Q_{loss}	*AVDI*	*VSI*
33-bus	88.268	61.175	0.8222	0.0030
69-bus	183.324	82.039	0.5703	0.0035

Table 7. Comparative Study (Scenario-3)

System	**Method**	**RGDs**	P_{loss}
		(kW/bus #)	(kW)
33-bus	IPOA [21]	801.7/13 1091.33/24 1053.64 /30	72.79
	AOA [22]	776.4/14 1099/24 1070.2/30	72.79
	A-FLO	1091.304/13 801.349/24 1054.11/30	72.787
69-bus	IPOA [21]	380.43/18 1718.97/61 526.75/11	69.4262
	AOA [22]	571.6/11 1719.9/61 341/21	69.43
	EPFA [17]	381.45/17 1718.84/61 525.56/11	69.43
	A-FLO	527.054/11 379.53/18 1719.428/61	69.428

Table 8. Simulations on 118-bus EDN

Item	HHO	HOA	PLO	A-FLO
P_{loss}	625.39	625.37	626.71	617.50
Q_{loss}	474.45	474.44	461.58	455.49
V_{min}	0.944/54	0.944/54	0.944/54	0.954/54
AVDI	0.00074	0.00074	0.00078	0.00072
VSI	0.6557	0.6556	0.6556	0.6557
DG	11141.96	11096.18	12041.51	11380.89
Best	625.39	625.37	626.71	617.50
Worst	840.95	812.04	842.71	863.60
Mean	664.41	650.44	675.93	646.47
Median	667.09	632.15	674.52	628.98
Std	34.68	36.67	35.58	31.22
Time	65.7047	66.3859	67.1359	62.1754

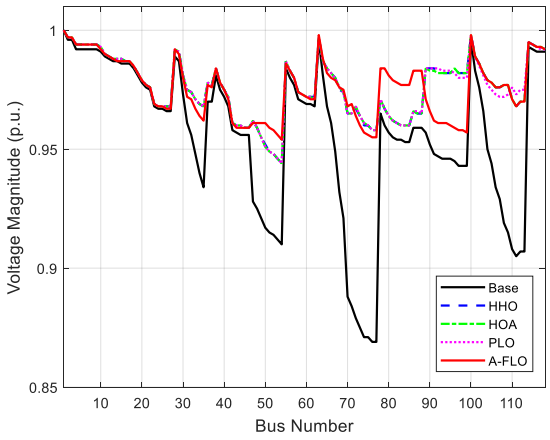

Fig. 2. Voltage profile of IEEE 118-bus

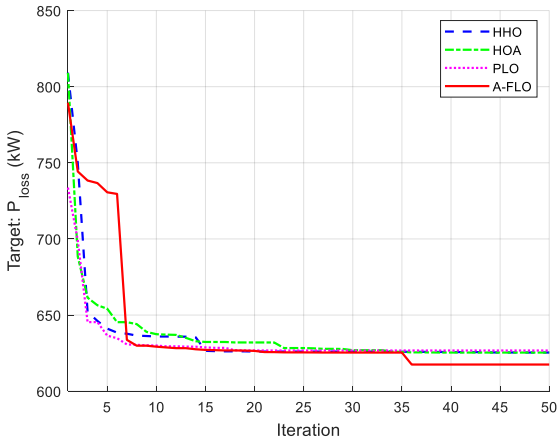

Fig. 3. Convergence curves for IEE 118-bus (Scenario-3)

In terms of robustness and consistency, A-FLO achieved the lowest best (617.50 kW), mean (646.47 kW), median (628.98 kW), and standard deviation (31.22 kW) of real power loss across all runs, highlighting its reliable convergence. Furthermore, A-FLO recorded the least execution time (62.1754 seconds), demonstrating computational efficiency alongside solution quality. The voltage profile and convergence curves for the best results are given in Fig. 2 and Fig. 3, respectively.

6 Conclusion

This study introduced Adaptive Frilled Lizard Optimization (A-FLO), a novel bio-inspired algorithm for the optimal integration of distributed generators (DGs) and fast-charging stations (FCSs) in distribution networks. By dynamically adjusting its exploration and exploitation phases, A-FLO effectively addresses the limitations of conventional metaheuristics, such as premature convergence and local optima trapping. Simulation results across the

IEEE 33-bus, 69-bus, and 118-bus test systems validate the superior performance of A-FLO: In the 33-bus system, real power loss reduced from 336.392 kW (with 50% EV load) to 250.516 kW after FCS integration, and further to 88.268 kW upon adding PV-based DGs. Voltage stability index (VSI) improved from 0.0139 to 0.00298, and minimum voltage increased from 0.8793 p.u. to 0.9743 p.u. In the 69-bus system, losses dropped from 345.376 kW to 225.124 kW with FCSs, and further to 183.324 kW with PV-DGs. VSI improved from 0.0057 to 0.00355, with minimum voltage rising from 0.8888 p.u. to 0.9165 p.u. For the 118-bus system, A-FLO outperformed HHO, HOA, and PLO with the lowest real power loss (617.50 kW), lowest standard deviation (31.22), and shortest computational time (62.17 s) across 50 independent runs. It also achieved the highest minimum voltage (0.954 p.u.) and the lowest AVDI (0.00072), reflecting enhanced voltage regulation. These results confirm that A-FLO not only enhances voltage stability and loss minimization but also scales efficiently to large networks with high penetration of renewable energy and EV infrastructure. Its adaptability and robustness make it a promising optimization tool for real-world smart grid applications.

Notation List

P_j^{new}	:	Real power load with CS/DG
P_j^{old}	:	Real power load at base case
Q_j^{new}	:	Reactive power load with CS/DG
Q_j^{old}	:	Reactive power load at base case
$P_{CS,j}$	:	Real power demand of CS
$P_{DG,j}$	:	Real power generation by DG
$Q_{CS,j}$	:	Reactive power demand of CS
$Q_{DG,j}$	:	Reactive power generation by DG
$\emptyset_{ev,i}$	:	Power factor of EV charger
$\emptyset_{dg,i}$	:	Power factor of DG power converter
ρ_i	:	Resistance of branch $i(\Omega)$
P_{loss}	:	Total Real power loss
$\|V_i\|$	:	Voltage magnitude of bus *i*
$AVDI$	:	Average voltage deviation index
v_{SI}	:	Voltage stability index
$\|V_r\|$	:	Nominal voltage
Z_i	:	Impedance of branch *i*
P_i	:	Real power demand at bus *i*
V_{min}	:	Minimum voltage limit
V_{max}	:	Maximum voltage limit
N_{br}	:	Total number of branches
$P_{D,base}$	:	Total real power load at base case
$Q_{D,base}$	:	Total reactive power load at base case
$P_{D,new}$	:	Total real power load with CS/DG
$Q_{D,new}$	:	Total reactive power load with CS/DG
N_{CS}	:	Number of CSs
N_{dg}	:	Number of DGs
N_{br}	:	Total number of branches
N_{bus}	:	Total number of buses

Conflicts of Interest

The authors declare no conflict of interest.

Author Contributions

Conceptualization, S.T. and V.R.A.; methodology, S.T.; software, I.A.; validation, S.T., R.G., and J.V.N.R.; formal analysis, S.T.; investigation, S.T.; resources, S.T.; data curation, S.T.; writing-original draft preparation, S.T.; writing-review and editing, V.R.A.; visualization, I.A.; supervision, R.G.; project administration, J.V.N.R.; funding acquisition, L.U.

References

[1] F. Ahmad, A. Iqbal, I. Ashraf, and M. Marzband, "Optimal location of electric vehicle charging station and its impact on distribution network: A review", *Energy Reports*, Vol. 8, pp. 2314-2333, 2022, doi: 10.1016/j.egyr.2022.01.180.

[2] A. Ghasemi-Marzbali, "Fast-charging station for electric vehicles, challenges and issues: A comprehensive review", *Journal of Energy Storage*, Vol. 49, p. 104136, 2022, doi: 10.1016/j.est.2022.104136.

[3] M. Abdel-Basset, A. Gamal, I. M. Hezam, and K. M. Sallam, "Sustainability assessment of optimal location of electric vehicle charge stations: a conceptual framework for green energy into smart cities", *Environment, Development and Sustainability*, Vol. 26, No. 5, pp. 11475-11513, 2024, doi: 10.1007/s10668-023-03373-z.

[4] F. Ahmad, A. Iqbal, I. Ashraf, M. Marzband, and I. Khan, "Placement of electric vehicle fast charging stations in distribution network considering power loss, land cost, and electric vehicle population", *Energy Sources, Part A: Recovery, Utilization, and Environmental Effects*, Vol. 44, No. 1, pp. 1693-1709, 2022, doi: 10.1080/15567036.2022.2055233.

[5] Y. Jin, M. A. Acquah, M. Seo, and S. Han, "Optimal siting and sizing of EV charging station using stochastic power flow analysis for voltage stability", *IEEE Transactions on Transportation Electrification*, Vol. 10, No. 1,

pp. 777-794, 2023, doi: 10.1109/TTE.2023.3275080.

[6] M. Nurmuhammed, O. Akdağ, and T. Karadağ, "A novel modified Archimedes optimization algorithm for optimal placement of electric vehicle charging stations in distribution networks", *Alexandria Engineering Journal*, Vol. 84, pp. 81-92, 2023, doi: 10.1016/j.aej.2023.10.055.

[7] M. A. Abdelaziz, A. A. Ali, R. A. Swief, and R. Elazab, "A reliable optimal electric vehicle charging stations allocation", *Ain Shams Engineering Journal*, Vol. 15, No. 7, p. 102763, 2024, doi: 10.1016/j.asej.2024.102763.

[8] A. K. Yousuf, Z. Wang, R. Paranjape, and Y. Tang, "An in-depth exploration of electric vehicle charging station infrastructure: A comprehensive review of challenges, mitigation approaches, and optimization strategies", *IEEE Access*, 2024, doi: 10.1109/ACCESS.2024.3385731.

[9] S. Muthukannan and D. Karthikaikannan, "Multiobjective planning strategy for the placement of electric-vehicle charging stations using hybrid optimization algorithm", *IEEE Access*, Vol. 10, pp. 48088-48101, 2022, doi: 10.1109/ACCESS.2022.3168830.

[10] M. Altaf, M. Yousif, H. Ijaz, M. Rashid, N. Abbas, M. A. Khan, M. Waseem, and A. M. Saleh, "PSO-based optimal placement of electric vehicle charging stations in a distribution network in smart grid environment incorporating backward forward sweep method", *IET Renewable Power Generation*, Vol. 18, No. 15, pp. 3173-3187, 2024, doi: 10.1049/rpg2.12916.

[11] N. Dharavat, S. K. Sudabattula, S. Velamuri, S. Mishra, N. K. Sharma, M. Bajaj, E. Elgamli, M. Shouran, and S. Kamel, "Optimal allocation of renewable distributed generators and electric vehicles in a distribution system using the political optimization algorithm", *Energies*, Vol. 15, No. 18, p. 6698, 2022, doi: 10.3390/en15186698.

[12] A. Ali, M. F. Shaaban, A. S. Awad, M. A. Azzouz, M. Lehtonen, and K. Mahmoud, "Multi-objective allocation of EV charging stations and RESs in distribution systems considering advanced control schemes", *IEEE Transactions on Vehicular Technology*, Vol. 72, No. 3, pp. 3146-3160, 2022, doi: 10.1109/TVT.2022.3218989.

[13] F. Ahmad, I. Ashraf, A. Iqbal, M. Marzband, and I. Khan, "A novel AI approach for optimal deployment of EV fast charging station and reliability analysis with solar based DGs in distribution network", *Energy Reports*, Vol. 8, pp. 11646-11660, 2022, doi: 10.1016/j.egyr.2022.09.058.

[14] A. Pratap, P. Tiwari, R. Maurya, and B. Singh, "Minimisation of electric vehicle charging stations impact on radial distribution networks by optimal allocation of DSTATCOM and DG using African vulture optimisation algorithm", *International Journal of Ambient Energy*, Vol. 43, No. 1, pp. 8653-8672, 2022, doi: 10.1080/01430750.2022.2103731.

[15] A. Pal, A. Bhattacharya, and A. K. Chakraborty, "Placement of electric vehicle charging station and solar distributed generation in distribution system considering uncertainties", *Scientia Iranica*, Vol. 30, No. 1, pp. 183-206, 2023, doi: 10.24200/sci.2021.56782.4908.

[16] T. Yuvaraj, K. R. Devabalaji, S. B. Thanikanti, V. B. Pamshetti, and N. I. Nwulu, "Integration of electric vehicle charging stations and DSTATCOM in practical Indian distribution systems using bald eagle search algorithm", *IEEE Access*, Vol. 11, pp. 55149-55168, 2023, doi: 10.1109/ACCESS.2023.3280607.

[17] T. K. Pandraju and V. Janamala, "An enhanced pathfinder algorithm for optimal integration of solar photovoltaics and rapid charging stations in low-voltage radial feeders", *Journal of Solar Energy Research*, Vol. 8, No. 4, pp. 1680-1690, 2023, doi: 10.22059/jser.2023.359041.1300.

[18] K. Kathiravan and P. N. Rajnarayanan, "Application of AOA algorithm for optimal placement of electric vehicle charging station to minimize line losses", *Electric Power Systems Research*, Vol. 214, p. 108868, 2023, doi: 10.1016/j.epsr.2022.108868.

[19] M. Bilal, F. Ahmad, and M. Rizwan, "Techno-economic assessment of grid and renewable powered electric vehicle charging stations in India using a modified metaheuristic technique", *Energy Conversion and Management*, Vol. 284, p. 116995, 2023, doi: 10.1016/j.enconman.2023.116995.

[20] S. L. Pappu, V. Janamala, and A. S. Veerendra, "Hunter–Prey Optimization Algorithm for Optimal Allocation of PV, DSTATCOM, and EVCS in Radial Distribution Systems", *Advanced Control for Applications: Engineering and Industrial Systems*, Vol. 6, No. 4, p. e231, 2024, doi: 10.1002/adc2.231.

[21] N. K. Ch, M. Thula, and J. Ch, "Improved Pufferfish Optimization Algorithm for Optimal Allocation of Photovoltaic Fast Charging Stations in Radial Distribution System",

International Journal of Intelligent Engineering & Systems, Vol. 18, No. 2, 2025, doi: 10.22266/ijies2025.0331.41.

[22] N. Pamuk, and U. E. Uzun, "Optimal allocation of distributed generations and capacitor banks in distribution systems using arithmetic optimization algorithm", *Applied Sciences*, Vol. 14, No. 2, 831, 2024, doi: 10.3390/app14020831.

[23] K. Subbaramaiah, P. Sujatha, "Optimal DG unit placement in distribution networks by multi-objective whale optimization algorithm & its techno-economic analysis", *Electric Power Systems Research*, Vol. 214, e108869, 2023, doi: 10.1016/j.epsr.2022.108869.

[24] N. M. Manousakis, P. S. Karagiannopoulos, G. J. Tsekouras, and F. D. Kanellos, "Integration of renewable energy and electric vehicles in power systems: a review", *Processes*, Vol. 11, No. 5, p. 1544, 2023, doi: 10.3390/pr11051544.

[25] T. Yuvaraj, K. R. Devabalaji, J. A. Kumar, S. B. Thanikanti, and N. I. Nwulu, "A comprehensive review and analysis of the allocation of electric vehicle charging stations in distribution networks", *IEEE Access*, Vol. 12, pp. 5404-5461, 2024, doi: 10.1109/ACCESS.2023.3349274.

[26] V. Tomar, M. Bansal, and P. Singh, "Metaheuristic algorithms for optimization: A brief review", *Engineering Proceedings*, Vol. 59, No. 1, p. 238, 2024, doi: 10.3390/engproc2023059238.

[27] I. A. Falahah, O. Al-Baik, S. Alomari, G. Bektemyssova, S. Gochhait, I. Leonova, O. P. Malik, F. Werner, and M. Dehghani, "Frilled Lizard Optimization: A Novel Bio-Inspired Optimizer for Solving Engineering Applications", *Computers, Materials & Continua*, Vol. 79, No. 3, 2024, doi: 10.32604/cmc.2024.053189.

[28] A. A. Heidari, S. Mirjalili, H. Faris, I. Aljarah, M. Mafarja, and H. Chen, "Harris hawks optimization: Algorithm and applications", *Future generation computer systems*, Vol. 97, pp. 849-872, 2019, doi: 10.1016/j.future.2019.02.028.

[29] S. O. Oladejo, S. O. Ekwe, and S. Mirjalili, "The Hiking Optimization Algorithm: A novel human-based metaheuristic approach", *Knowledge-Based Systems*, Vol. 296, p. 111880, 2024, doi: 10.1016/j.knosys.2024.111880.

[30] C. Yuan, D. Zhao, A. A. Heidari, L. Liu, Y. Chen, and H. Chen, "Polar lights optimizer: Algorithm and applications in image segmentation and feature selection", *Neurocomputing*, Vol. 607, 128427, 2024, doi: 10.1016/j.neucom.2024.128427.